Supporting Appendix

Availability of public goods shapes the evolution of competing metabolic strategies

Short title:
Growth in isolation favors increased efficiency

Herwig Bachmann[a,b,c,1] Martin Fischlechner[d,e], Iraes Rabbers[a], Nakul Barfa[a,b], Filipe Branco dos Santos[a,b], Douwe Molenaar[a,b], Bas Teusink[a,b,1]

[a] Systems Bioinformatics IBIVU, Amsterdam Institute for Molecules Medicines and Systems, Vrije Universiteit Amsterdam, De Boelelaan 1085, Amsterdam 1081 HV, The Netherlands.
[b] Kluyver Centre for Genomics of Industrial Fermentation / NCSB, Julianalaan 67, 2628 BC Delft, The Netherlands.
[c] NIZO Food Research and Top Institute Food and Nutrition, Kernhemseweg 2, 6718ZB Ede, The Netherlands.
[d] Chemistry, and [e]Institute for Life Sciences, University of Southampton, Highfield Campus, Southampton SO17 1BJ, United Kingdom.

[1] To whom correspondence may be addressed. E-mail: h.bachmann@vu.nl or b.teusink@vu.nl

SI Appendix: Text

Yield/rate trade-off

Well-described examples of a yield/rate trade-off are the ones dealing with metabolic shifts in central carbon metabolism. For instance the Crabtree effect in yeast describes that an increase of the growth rate leads to production of ethanol even in the presence of sufficiently high oxygen concentrations. Such a shift from respiration to fermentation causes large differences in ATP and biomass yield (32 mol ATP per glucose versus 2 mol ATP per glucose, respectively)(1). Other examples for such a trade-off are the shift from acetate production to lactate production in lactic acid bacteria (2), the production of acetate by *E. coli* (3) at high growth rates and also the Warburg effect in cancer cells (4).

Although these examples demonstrate such a trade-off, several attempts to evolve organisms with an increased yield failed. Next to the examples mentioned in the main text, the yield/rate trade-off was studied in *E. coli* evolving in the laboratory for 20000 generations. In this study the authors did not find a trade-off when comparing evolved strains with their ancestors or across independently evolved populations (5). However, within three out of four evolved populations they did find a significant negative correlation between yield and rate. The authors speculate that the failure to observe a trade-off in the first two comparisons could be due to incomplete adaptation to the growth medium when they started the experiment or because the maximum possible growth rate was attained, which would hamper the detection of a yield-rate trade-off. The authors do acknowledge limitations of their experimental setup that possibly compromise the detection of such a trade-off, and suggest dedicated experiments for further investigation.

MacLean (6) compared the glucose uptake rate and the biomass yield of 13 different yeasts from the *Saccharomyces* clade (data obtained from Merico *et al.* (7)). After the omission of 2 strains that did not produce ethanol, a significant negative correlation was found between the glucose uptake rate and the biomass yield. However, when the actual growth rate measured in the same experiment is compared to the biomass yield, this correlation does not exist anymore (SI Appendix; Fig. S12). From an evolutionary perspective the growth rate is much more relevant to the yield-rate trade-off than the glucose uptake rate. The reason for this discrepancy between glucose uptake and growth rate might lie in the fact that most of these strains are not optimized for growth in the medium that this data was obtained in. Depending on how well a strain was adapted to the particular medium, the actual yield ratio could be far away from optimality, which makes it impossible to identify a yield/rate trade-off line.

Microbial growth in emulsion

In our study emulsions were generated by mechanically shaking growth medium with the appropriate cell density with suitable oil supplemented with a surfactant. The resulting emulsions droplets are polydisperse (droplets vary in diameter) and for our experiments we assumed an average droplet size of 50 μm (Figure S1). The size distribution of droplets did not change during at least three days of incubation, indicating that droplet fusion does not occur or is very limited. An average droplet size of 50 μm corresponds to a droplet volume of 65 picoliters. Based on the average droplet size, the prepared emulsions contained approximately 4.6 million droplets. As we used 300 μl of medium containing 2×10^6 cells per ml to prepare the emulsions the expected number of cells per droplet is approximately $(2\times10^6 \times 0.3)/4.6\times10^6 = 0.13$. Assuming that droplet occupation follows a Poisson distribution, it was calculated that 11.4% of all droplets were filled with a single cell and that less than 1% were occupied with more than one cell (Figure S1). Droplets with a smaller diameter have a smaller likelihood of being occupied by a cell and because the volume of a sphere scales with the third power of the radius smaller droplets form a relatively small fraction of the total volume. Bigger droplets are more likely to be occupied by more than one cell. Such droplets would not contribute to the selection of cells with an increased number of offspring if they co-reside in a droplet with a faster growing strain. This means that droplets with a large diameter will slow down the selection process but will not be detrimental to it. Based on an average droplet volume of 65 picoliters, an initial cells density of 1 cell per droplet and a maximum cell density of 1×10^9 cell/ml the number of cell divisions in a fully-grown droplet is approximately 6.

Lactococcus lactis MG1363 can also form short chains of bacteria, which could lead to the inoculation of individual droplets with more than one cell. Since cells within a chain are likely to be genetically identical, this effect should not compromise the selection procedure.

To estimate the number or transfers in emulsion required to identify mutant strains we assumed that one in a million cells carries a mutation leading to an increased number of offspring. If the increase in the number of offspring is 30% the enrichment of this mutant will be more than three orders of magnitude within 30 transfers. If the increase in the number of offspring is 50% the enrichment after 30 transfers will be more than five orders of magnitude, which would render it making up more than 10 percent of the total population.

Serial propagation in emulsion allows selection for an increased number of offspring: Proof of principle

We used the protocol for serial propagation in emulsion to propagate *L. lactis*, a lactic acid bacterium that produces mainly lactate as a metabolic end product. In

L. lactis the production of acetate yields 50% more ATP compared to the production of lactate as a metabolic end product (Fig. 1). Consistent with a suggested yield/rate trade-off in organisms a lactate dehydrogenase (*ldh*) mutant, in which the glycolytic flux is mainly diverted towards acetate production, grows almost 4-fold slower but reaches 30% higher cell densities than the wild type strain (8). In a proof of principle assay we showed that in competition with the wild type strain the fraction of the slow but efficient *ldh* mutant increased if propagated in emulsion, while it rapidly decreased in suspension (Fig. 1).

Serial propagation of *L. lactis* in emulsion selects for populations with an increased number of offspring

In the main text we describe the selection of a high-yield mutant (HB60) through serial propagation in emulsion. However, a competition experiment of HB60 and the wild type strain MG1363 propagated in emulsion every second day resulted in the co-existence of the two strains but the fraction of HB60 did not increase. This was an unexpected result, as we selected HB60 using this same selection scheme. We hypothesized that the survival of HB60 in emulsion was lower than that of MG1363. Subsequent experiments revealed that variants with elevated final optical densities increased in frequency in the initial emulsion if the propagation was continued (Fig. 2) and that HB60 could invade the wild type population in emulsion when propagated every day, rather than every two days (SI Appendix; Fig. S3). These results corroborate the notion that the survival of HB60 compared to MG1363 in emulsion is compromised and that the initial EMS-mutagenized population contained no or very few wild type variants. The suggestion that very few or no wild type variants resided in the EMS-mutagenized population of MG1363 is further supported by two populations of EMS-treated MG1363 that were adapted in suspension for 120 generations. This is comparable to the number of generations during the 22 propagation steps in emulsion (~6 divisions per emulsion step). The suspension adapted populations MG1363_Sus1 and MG1363_Sus2 showed both a lower growth rate and yield than the wild type MG1363 (SI Appendix; Fig. S10).

Full genome re-sequencing

Full genome re-sequencing revealed that strain HB60 contained one point mutation in *ptnD* (see main text and Figs. S6, S8, S9) but also 3 loci where a mobile genetic element inserted into the genome. Transposable element IS*981* inserted into either *i)* the intergenic region between a hypothetical protein and the 50s ribosomal protein L10 *ii)* into the coding region of a hypothetical protein and *iii)* in the intergenic region of two genes encoding hypothetical proteins (Table S2). All three insertions were also found back in strains HB61 and HB62.

We cannot exclude that these insertions have an effect on the observed phenotype of HB60. However, the fact that in strains HB61 and HB62 three independent events led to the emergence of new promoters upstream of glucose transporters, indicate the importance of glucose transport for the selected phenotypes. It furthermore corroborates the importance of the identified mutation in the glucose transporter subunit *ptnD* in HB60. For its validation we tested a MG1363 derived strain in which the complete glucose transport system *ptnABCD* is deleted (NZ9000Δ*ptn*ABCD). This strain showed indeed a growth rate and growth yield similar to the one of HB60 (SI Appendix; Fig. S10). The serial propagation of NZ9000Δ*ptn*ABCD in suspension led to an increased growth rate and a decreased yield resembling the trajectories seen with the HB60 reversions towards HB61, HB62 and HB63.

SI Appendix: Tables

Table S1: Strains used in this study

Strain	Description	Reference
MG1363	*L. lactis* plasmid and phage cured derivative of NCDO712	Gasson 1983, Wegmann *et al.* 2007
NZ9000	*pepN::nisRK* derivative of *L. lactis* MG1363	Kuipers *et al.* 1997
NZ9010	*ldh::ery* derivative of *L. lactis* NZ9000; *ldh* negative strain that reverts to a Ldh positive phenotype through the activation of *ldhB* (Bongers *et al.* 2003)	Hoefnagel et al. 2002
NZ9020	*ldh::ery; ldh*B*::tet* derivative of L. lactis NZ9000; double mutant of *ldh* and *ldh*B in NZ9000	Bongers et al. 2003
NZ9000*ΔptnABCD*	Derivative of NZ9000 containing a 1736-bp deletion in *ptnABCD*	Pool *et al.* 2006
NZ9000*ΔptcBA*	Derivative of NZ9000 containing a deletion in *ptnBA*	Pool *et al.* 2006
HB60	MG1363 derivative selected after propagation in emulsion; shows a slow growth and high yield phenotype;carries a F65L mutation in *ptnD*	this study
HB61	HB60 derivative selected after propagation in suspension; shows a growth rate and growth yield phenotype similar to MG1363; carries IS905 upstream of the *ptnABCD* operon	this study
HB62	HB60 derivative selected after propagation in suspension; shows a growth rate and growth yield phenotype similar to MG1363	this study
HB63	HB60 derivative selected after propagation in suspension; shows a growth rate and growth yield phenotype similar to MG1363; carries IS905 upstream of the *ptnABCD* operon and IS905 upstream of *glcU*	this study

Table S2: Genome re-sequencing revealed three re-arrangements in HB60 and the additional insertions of IS*905* upstream of *ptnABCD* and *glcU* in strains HB61 and HB63.

Identified rearrangement	Insertion locus	Position of Insertion[2]	Insertion length(bp)[2]	detected in HB60	detected in HB61	detected in HB63
ps435::IS905[1]	intergenic	2090433	1316	yes	yes	yes
llmg_1205/rplJ::IS981	intergenic	1175482	1231	yes	yes	yes
llmg1411::pseudo13..IS981	in coding region	1379183	2256	yes	yes	yes
ps507/ps506::IS981	intergenic	2221296	1228	yes	yes	yes
ptnAB/fer::IS905	intergenic	712501	1316	no	yes	yes
glcU/llmg_2562::IS905	intergenic	2521652	1326	no	no	yes

[1] This rearrangement does not occur in the published genome of *L. lactis* MG1363 but it was found in the isolate that we started all experiments with (designated Gen0).

[2] IS*905* and IS*981* occur 14 and 16 times in the genome of MG1363 respectively (Accession: NC_009004). Depending on the mapping of our reads with the different IS elements the insertion position and insertion length can vary by a number of bases.

SI Appendix: Figures

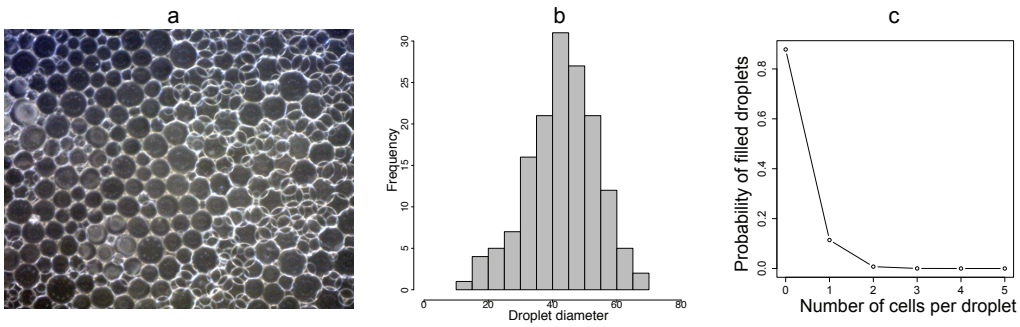

Figure S1

Emulsion droplets as prepared for the compartmentalized propagation of microbial cells (panel a). A histogram of the droplet diameters of 152 droplets from the picture in panel a (manually measured with ImageJ; http://imagej.nih.gov/ij/, 1997-2012) shows a mean droplet diameter of 43 µm (panel b), which equals a volume of 42 picoliter. Based on the average droplet size cell densities for droplet generation can be calculated. Droplet occupation will follow a probability distribution as shown in panel c (valid for a monodisperse emulsion (uniform droplet diameter)). Droplet size can slightly vary between different emulsions. Typically we saw the majority of droplet diameters ranging from 40-60 µm.

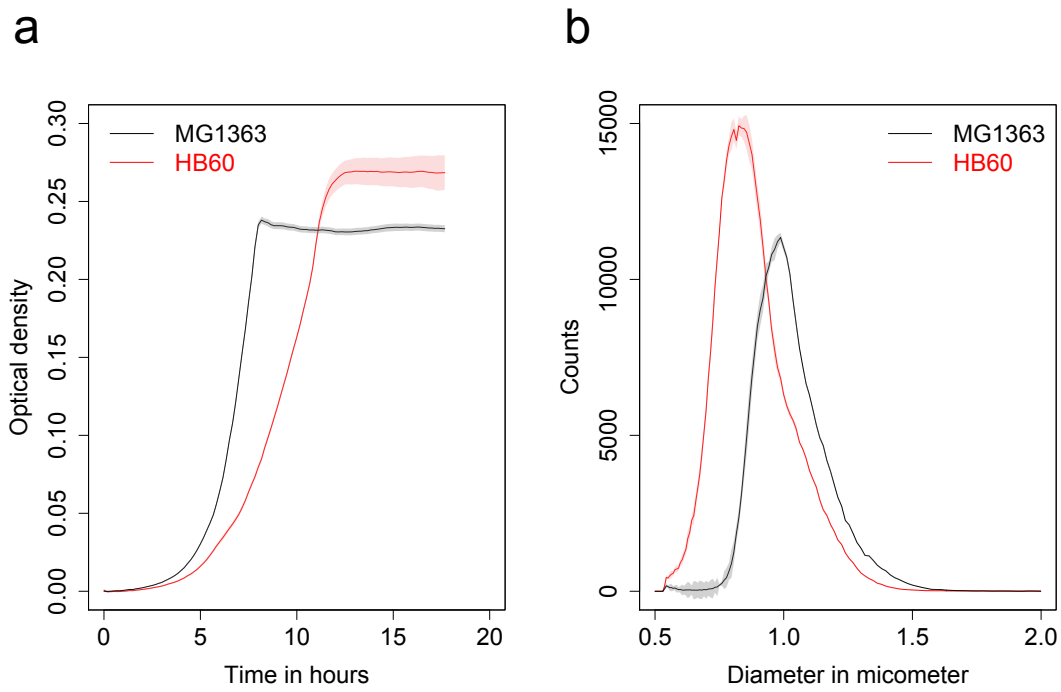

Figure S2

Growth curves (a) and cell size measurements (b) of strain HB60 (red) and MG1363 (black). The shaded areas indicate the SEM (n=12, panel a) (n=2, panel b). Please note that the emulsion based selection protocol selects for an increased number of viable offspring at the time of propagation and not necessarily for increased biomass yield. For instance a mutant with an increased number of viable offspring but decreased cell size and decreased total biomass would be favored by selection in emulsion. In the case of HB60 an increased number of offspring coincides with an increased biomass yield.

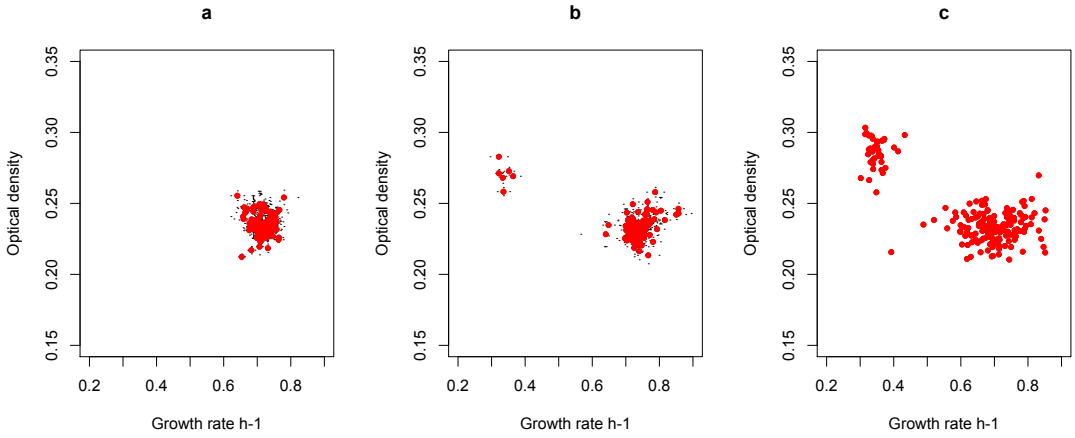

Figure S3

Invasion of the MG1363 wild type population by strain HB60. HB60 was mixed with MG1363 and propagated in emulsion every 24 hours. In the initial culture HB60 was not detected in 96 individual colonies (panel a). After 4 (panel b) and 8 transfers (panel c) in emulsion the fraction of HB60 increased as compared to the initial frequency in the population. The fraction of HB60 in the population is <1%, 6% and 23% in panel a, b and c respectively.

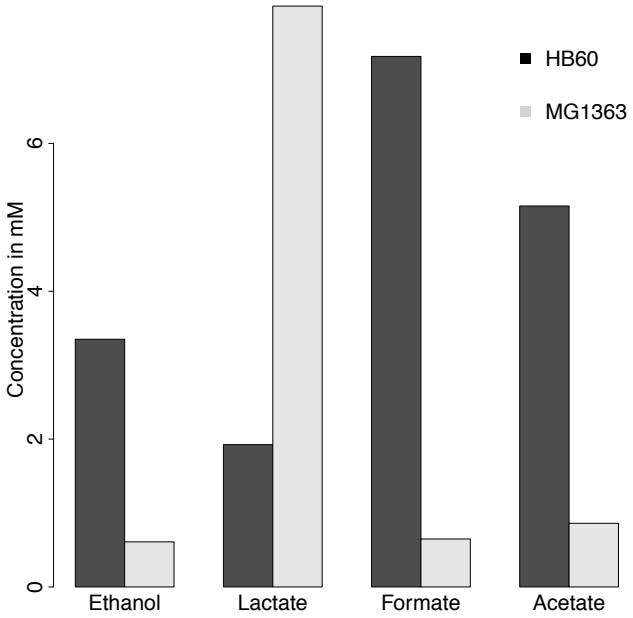

Figure S4

Organic acid profiles of strains MG1363 and HB60.

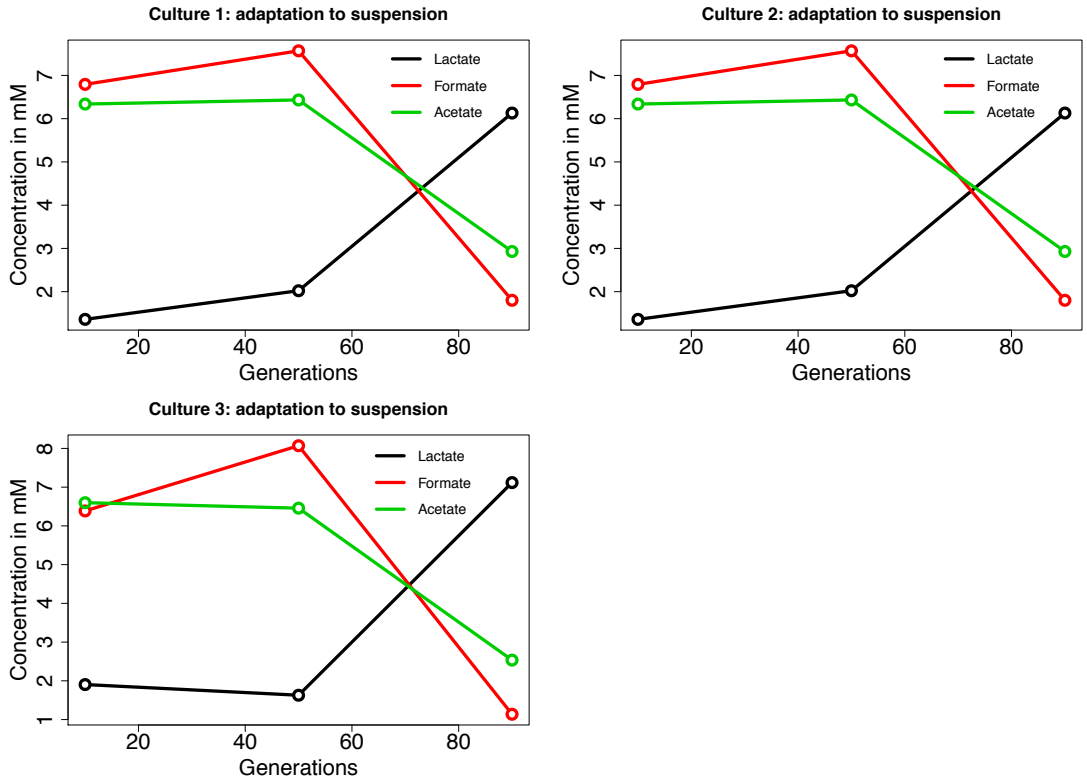

Figure S5

Organic acid profiles of HB60 (data points after 10 generations) and during its adaptation to growth in suspension for 50 and 90 generations. Three independent cultures were adapted in parallel (panels a, b and c) and from each culture a single colony was isolated and designated HB61, HB62 HB63 respectively. The organic acid profiles of the entire population after 90 generations resemble the profiles of the single colonies that were isolated.

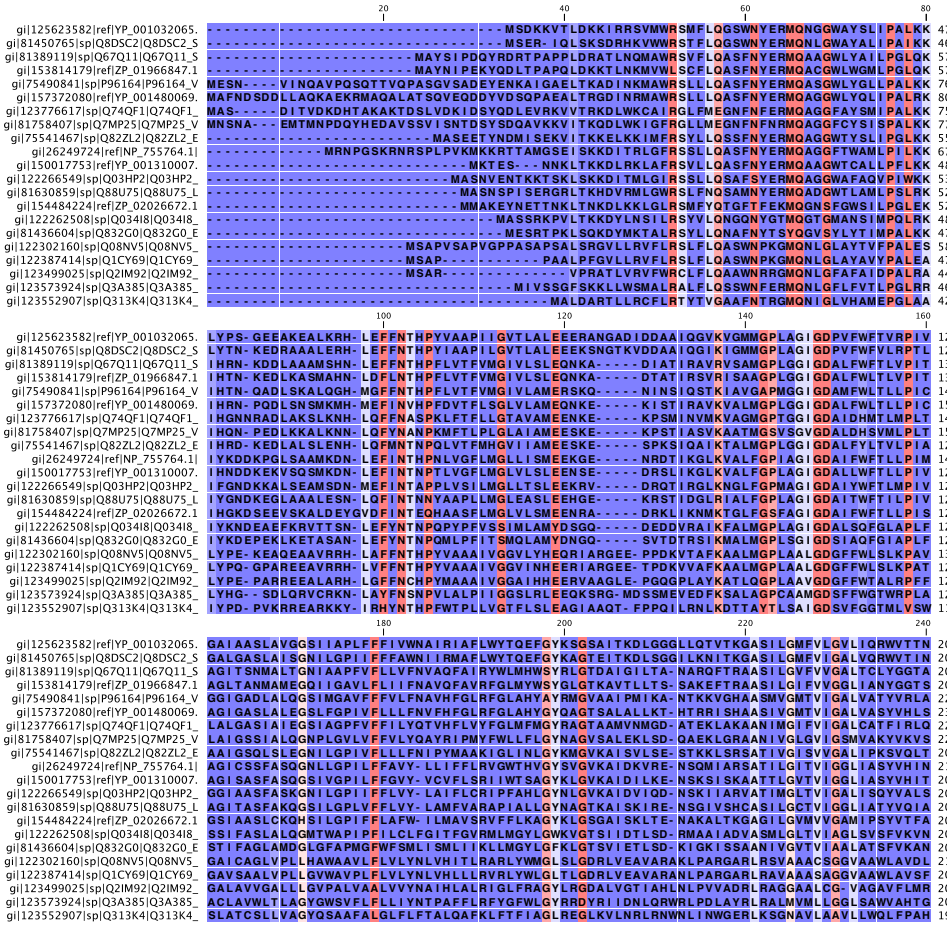

Figure S6

Protein alignment of the protein family pfam03613, which encodes the PTS system mannose/fructose/sorbose family IID component (only the first 240 residues of the alignment are shown). The alignment shows the PtnD protein of MG1363 (top row) and the 20 most diverse members of the protein family as selected by the NCBI CDD database (retrieved on 24th September 2012). The alignment was made in ClustalW with standard settings and visualization was done in CLC sequence viewer. Amino acid conservation is indicated from blue to red with an increasing degree of conservation. At position 100 of the alignment a phenylalanine (F) residue is indicated to be well conserved. The G→T mutation that occurred at position 710325 (GenBank NC_009004) during the adaptation in emulsion lead to a change from phenylalanine at this position in MG1363 to a leucine in HB60 (F65L). The overall conservation of a phenylalanine residue in the mutated position in 3256 proteins (http://pfam.sanger.ac.uk; 24Sep2012) of this family is 86%. The IID component of the PTS systems is located in the cell membrane and together with component IIC it is responsible for the translocation of sugar moieties over the membrane. Based on the observed decrease of the glycolytic flux in HB60 (SI Appendix; Fig. S7) we conclude that the F65L mutation led to decreased PtnD activity.

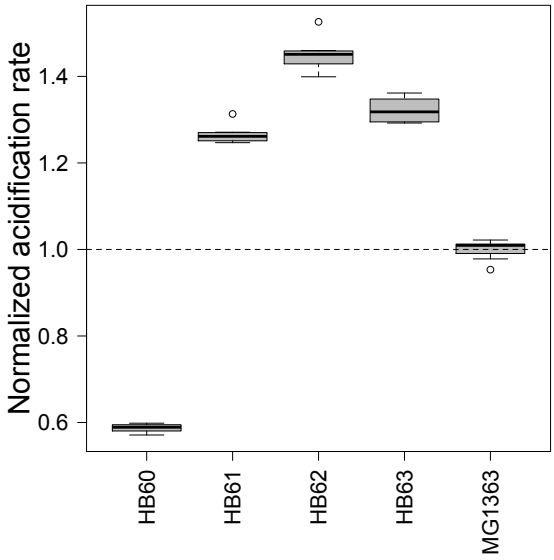

Figure S7

Acidification rate normalized to wild type strain MG1363. Major metabolic end products in *L. lactis* are lactic acid, acetic acid and formic acid, which contribute to the acidification of the medium. The acidification rate is therefore a readout for the glycolytic flux. Compared to the wild type, strain HB60 shows 41% decreased acidification rate, while HB61, HB62 and HB63 show a 27%, 32% and 45% increase in their acidification rate respectively. HB60 shows a different organic acid profile, which might lead to an overestimation of the corresponding glycolytic flux based on the acidification rate.

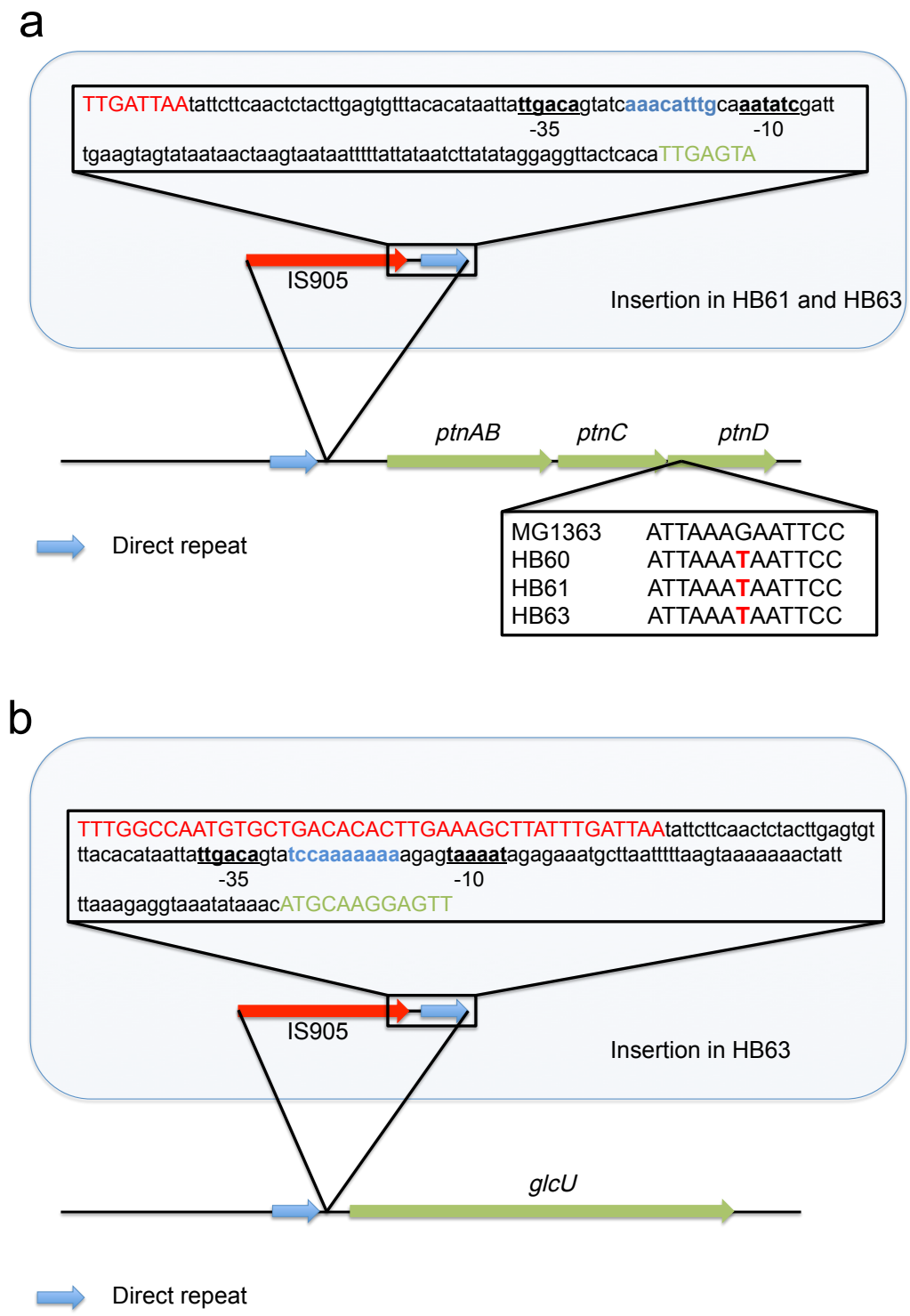

Figure S8

The selection of MG1363 in emulsion resulted in the isolation of a mutant (HB60) with a point mutation (F65L) in *ptnD*. During the subsequent adaptation of HB60 in suspension insertion element IS*905* (red) integrated into the

promoter region of the *ptnABCD* operon in strains HB61 and HB63. IS*905* carries a perfect, outward facing -35 promoter element (underlined). This -35 element in combination with the down-stream located -10 element (underlined) closely resembles a consensus promoter sequence that did not occur in the parent strain. The original point mutation found in *ptnD* of strain HB60 remained in strains HB61 and HB63 during the adaptation in suspension. The up-regulation of transcription through the insertion of IS*905* in promoter regions of MG1363 has been described before (9, 10). The insertion locus of IS*905* is flanked by direct terminal repeats (light blue). The IS element is inserted at position 712501 in the genome of *L. lactis* MG1363 (GenBank NC_009004)

Panel b: In HB63 IS*905* integrated also in the upstream region of the glucose permease gene *glcU*. Analogous to panel a this insertion resulted in the integration of the same -35 element (underlined) 17 bases upstream of a -10 element (underlined) which results in a region that closely resembles a consensus promoter sequence that did not occur in the parent strain. The IS element is inserted at position 2521652 in the genome of *L. lactis* MG1363 (GenBank NC_009004).

a

GAACAACTGTAATATTTTTATGAAAACATT**GGTAGTGTAAAATAAGTTGTGTAAACA**CTAAAAAGGAATAAATCCGTTAT
AGTAGAGTTGCGAAACATTACTAGAAAGAGATTTATTCCTATGACTCAGTTTACCACAGAACTACTTAACTTCCTAGCCCAAA
AGCAAGATATTGATGAATTTTTCCGTACTTCTCTTGAAACTGCTATGAATGATCTGCTTCAAGCAGAGTTATCAGCCTTTTTA
GGGTATGAACCTTACGATAAAGTAGGCTATAATTCTGGGAATAGTCGTAACGGAAGCTATTCACGGCAATTTGAAACCAAATA
TGGGACTGTTCAGTTGAGCATTCCTAGAGATCGTAATGGGAACTTTAGTCCAGCTTTGCTTCCCGCTTATGGACGTCGAGATG
ACCACTTGGAAGAGATGGTTATCAAACTCTATCAAACCGGTGTAACGACTCGAGAAATTAGTGATATCATCGAGCGAATGTAT
GGTCATCACTATAGTCCTGCCACAATTTCTAATATCTCAAAAGCAACTCAGGAGAATGTCGCTACTTTTCATGAGCGAAGCTT
AGAAGCCAATTACTCTGTTTTATTTCTTGACGGAACCTATCTTCCATTAAGACGTGGAACCGTTAGTAAAGAATGTATTCATA
TCGCACTTGGCATTACACCAGAAGGACAGAAGGCTGTTCTTGGATATGAAATCGCCCCAAATGAAAATAATGCTTCTTGGTCC
ACCCTGTTAGACAAGCTTCAAAACCAAGGAATCCAACAGGTTTCTCTTGTAGTGACCGATGGCTTCAAGGGGCTTGAACAGAT
TATCAGTCAGGCTTACCCATTAGCTAAACAACAACGTTGCTTAATTCATATTAGTCGAAATCTAGCTAGTAAAGTGAAACGAG
CAGATAGAGCGGTTATTCTGGAGCAATTTAAAACGATTTATCGTGCTGAAAATTTAGAAATGGCAGTGCAAGCTTTAGAGAA
CTTTATCGCCGAATGGAAACCAAAGTATAGGAAAGTCATGGAAAGTCTGGAGAATACGGATAATCTTTTAACTTTTTATCAGT
TTCCCTACCAGATTTGGCACAGCATTTATTCGACAAACCTCATTGAGTCTCTTAACAAAGAAATCAAACGTCAAACGAAAAAG
AAGGTTCTTTTTCCTAACGAGGAGGCTCTGGAACGTTACTTAGTTACTTTGTTTGAAGATTATAATTTCAAGCAAAGTCAACG
CATCCATAAAGGGTTTGGCCAATGTGCTGACACACTTGAAAGCTTATTTGATTAATATTCTTCAACTCTACTTGA**GTGTTTAC**
ACATAATTATTGACAGTATCAAACATTTGCAAATATCGATTTGAAGTAGTATAATAACTAAGTAATAATTTTTATTATAAT
CTTATATAGGAGGTTACTCACATTGAGTATCGGAATTGTTATTGCGAGCCATGGTGAATTCGCTGCAGGCATCAAACAATCTG
GTTCTATGATTTTCGGAGAGCAAGAAAAAGTACAAGTTGTTACTTTTATGCCTAGCGAAGGACCAACTGATTTGCATGCTAAA
ATTGAAGCTGCCATCGCAACATTTGATGCTGAAGATGAAGTACTTGTCCTTGCTGACTTATGGAGCGGTTCTCCATTTAACCA
AGCAAGTGCAGTGATGGGTGAAAATCCAGAGCGCAAGATCGCTATCATCACAGGCCTCAACCTGCCTATGCTTATCCAAGCCT
ACACAGAACGCATGATGGACGCGTCTGCTGGAGTGGATAAAGTCGTAGCAAATATTATGAAAGAAGCCAAAGGCGGTA

b

CGCCGCCAATTTTAGTTCTAATTGAAAAAAGAAAATAAATTTACTTGAACAGTTATGAATCTTATGTATTCTTTTATCTCTTG
TTTTTTCCAAAAAAA**GGTAGTGTAAAATAAGTTGTGTAAACA**CAAAAAGGAATAAATCCGTTATAGTAGAGTTGCGAAAC
ATTACTAGAAAGAGATTTATTCCTATGACTCAGTTTACCACAGAACTACTTAACTTCCTAGCCCAAAAGCAAGATATTGATGA
ATTTTTCCGTACTTCTCTTGAAACTGCTATGAATGATCTGCTTCAAGCAGAGTTATCAGCCTTTTTAGGGTATGAACCTTACG
ATAAAGTAGGCTATAATTCTGGGAATAGTCGTAACGGAAGCTATTCACGGCAATTTGAAACCAAATATGGGACTGTTCAGTTG
AGCATTCCTAGAGATCGTAATGGGAACTTTAGTCCAGCTTTGCTTCCCGCTTATGGACGTCGAGATGACCACTTGGAAGAGAT
GGTTATCAAACTCTATCAAACCGGTGTAACGACTCGAGAAATTAGTGATATCATCGAGCGAATGTATGGTCATCACTATAGTC
CTGCCACAATTTCTAATATCTCAAAAGCAACTCAGGAGAATGTCGCTACTTTTCATGAGCGAAGCTTAGAAGCCAATTACTCT
GTTTTATTTCTTGACGGAACCTATCTTCCATTAAGACGTGGAACCGTTAGTAAAGAATGTATTCATATCGCACTTGGCATTAC
ACCAGAAGGACAGAAGGCTGTTCTTGGATATGAAATCGCCCCAAATGAAAATAATGCTTCTTGGTCCACCCTGTTAGACAAGC
TTCAAAACCAAGGAATCCAACAGGTTTCTCTTGTAGTGACCGATGGCTTCAAGGGGCTTGAACAGATTATCAGTCAGGCTTAC
CCATTAGCTAAACAACAACGTTGCTTAATTCATATTAGTCGAAATCTAGCTAGTAAAGTGAAACGAGCAGATAGAGCGGTTAT
TCTGGAGCAATTTAAAACGATTTATCGTGCTGAAAATTTAGAAATGGCAGTGCAAGCTTTAGAGAACTTTATCGCCGAATGGA
AACCAAAGTATAGGAAAGTCATGGAAAGTCTGGAGAATACGGATAATCTTTTAACTTTTTATCAGTTTCCCTACCAGATTTGG
CACAGCATTTATTCGACAAACCTCATTGAGTCTCTTAACAAAGAAATCAAACGTCAAACGAAAAAGAAGGTTCTTTTTCCTAA
CGAGGAGGCTCTGGAACGTTACTTAGTTACTTTGTTTGAAGATTATAATTTCAAGCAAAGTCAACGCATCCATAAAGGGTTTG
GCCAATGTGCTGACACACTTGAAAGCTTATTTGATTAATATTCTTCAACTCTACTTGA**GTGTTTACACATAATTATTGACAG**
TATCCAAAAAAAAGAGTAAAATAGAGAAATGCTTAATTTTTAAGTAAAAAAACTATTTTAAAGAGGTAAATATAAACATGCA
AGGAGTTCTTCTCGCGCTTGTTCCAATGTTTGCTTGGGGTTCTATCGGATTTGTAGCTAACAAATTTGGTGGAGATGCTAAAC
AACAAACACTTGGAATGACATTAGGCGCTTTTGTTTTTGCACTTATTGTTTTCTTATTCCGTATGCCAACATTGACCATGGCA
AATTTTCTTAATTGGATTTATTGGTGGTTTACCTTTGGGCGATTGGTCAATTTGGTCA

Figure S9

Genomic region of the *ptn* locus after the IS*905* integration in strains HB61 and HB63. IS*905* is indicated in red and the partial *ptnA* gene in green (panel a). Genomic region of the *glcU* locus after the IS*905* integration in strain HB63. IS*905* is indicated in red and the partial *glcU* gene in green (panel b). The IS element is flanked by inverted repeats (10) which are underlined and in bold.

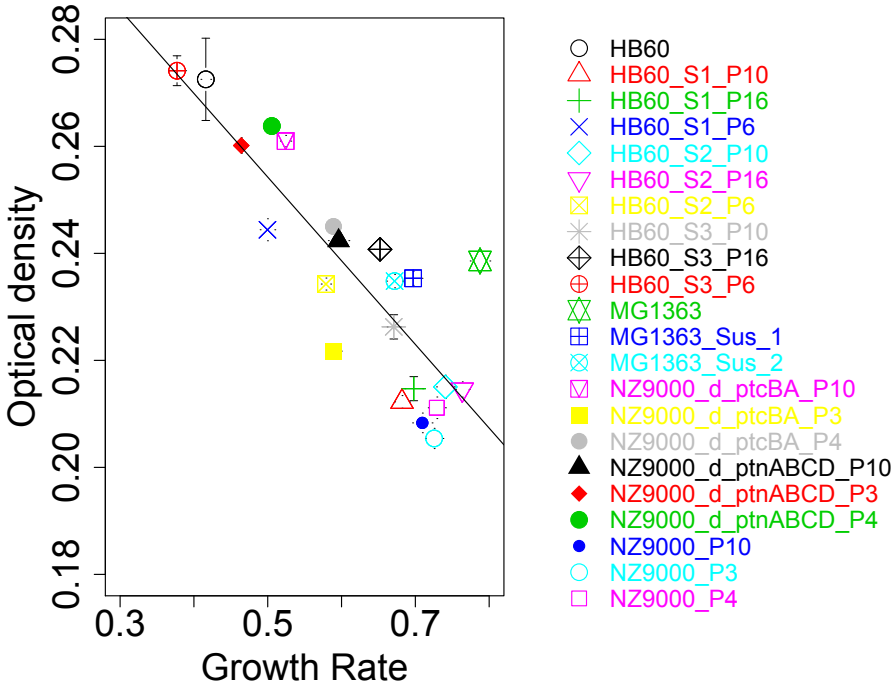

Figure S10

Yield/rate plot of *L. lactis* MG1363 and 21 derivatives. HB60–S1, HB60-S2 and HB60–S3 are individual cultures of HB60 that were adapted to growth in suspension for 60, 100 and 160 generations (legend designations end with -P6, -P10 and -P160 respectively). Strains HB60-S1-P10, HB60-S2-P10, HB60-S3-P10 are single colony isolates from the individual cultures and they were designated HB61, HB62 and HB63 respectively. MG1363_Sus_1 and MG1363_Sus_2 are cultures of the originally EMS treated MG1363 culture that was propagated for 120 generations in suspension. Strains NZ9000_*ΔptnABCD* (11) is deficient of the mannose PTS which was found to be mutated in HB60. Strain NZ9000_*ΔptcBA* (11) is deficient of a cellobiose PTS system that is also involved in glucose uptake in *L. lactis.* Strains NZ9000(12), NZ9000_*ΔptnABCD* and NZ9000_*ΔptcBA* were obtained on GM17 medium and adapted to growth in the chemically defined medium (CDMpc). The cultures indicated in this figure were adapted for 30, 40 and 100 generations (legend designations end with -P3, -P4 and -P10 respectively). Standard errors are shown (n=11). If error bars are not visible they fall within the plotted symbol. The diagonal line shows a linear regression line with an adjusted R^2= 0.71 and a p<0.0001, DF=20. From the same cultures cell size, cell numbers, organic acid profiles and the total protein content was determined. See the correlations in Fig. 4 of the main text.

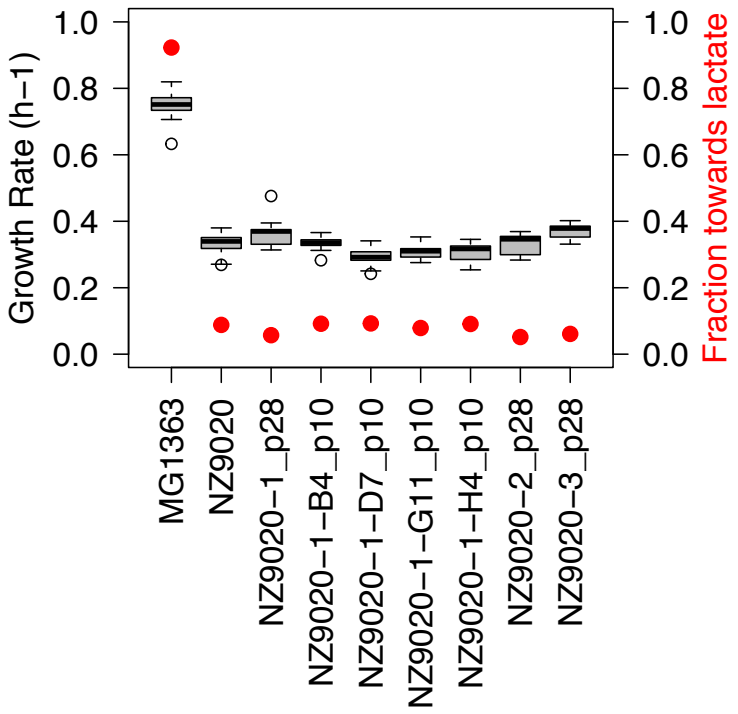

Figure S11

Serial propagation of the double *ldh* mutant NZ9020 for up to 280 generations did not result in an increased growth rate (primary y-axis) or a change in lactate production (secondary y-axis). NZ9020 was cultured for approximately 100 generations (culture designations ending with "-p10") or approximately 280 generations (culture designations ending with "-p28"). The propagation for 100 generations was done for 96 individual cultures with similar results for growth rates. MG1363 is shown as a reference.

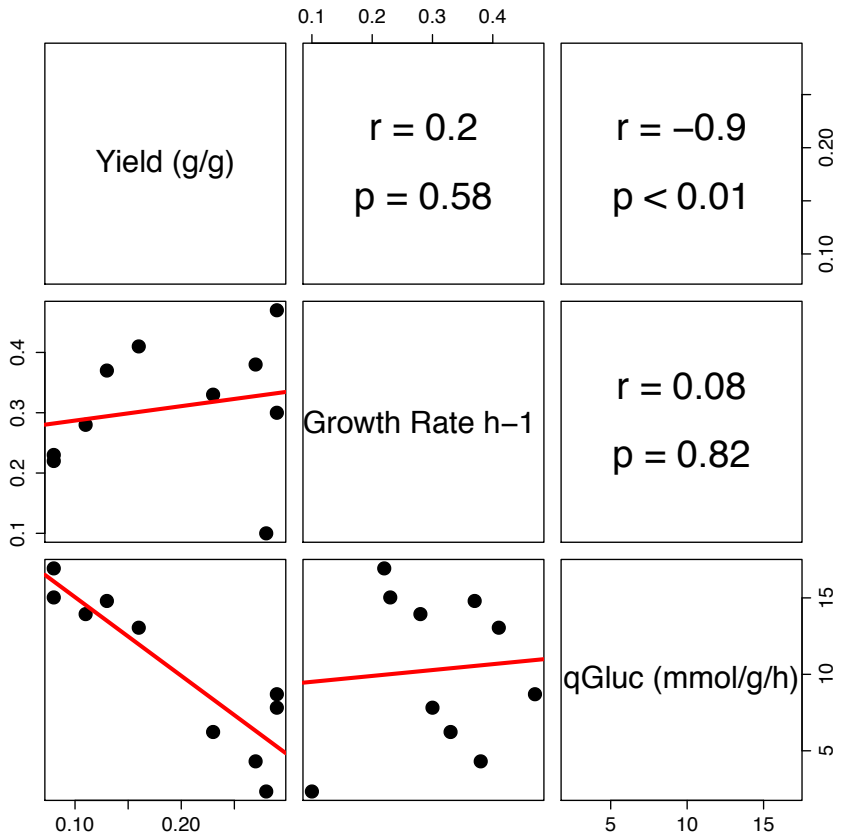

Figure S12

MacLean 2008 argued for the existence of a yield/rate trade-off based on the biomass/glucose uptake (qGluc) plot of different yeast species (bottom left panel). However, within the same dataset this correlation is not found if the growth rate is compared to either biomass yield or the glucose consumption rate, indicating that in yeasts there seems no clear correlation between growth rate and glucose uptake rate under these conditions as also observed by Youk *et al.* (13). Data taken from Merico *et al.* 2007 (7). Bottom panels show the individual data points fitted with a linear model (red line) and the top panels show the corresponding Pearson correlation coefficients and p-values.

SI Appendix: Materials and Methods

Chemically induced mutagenesis

For chemically induced mutagenesis *L. lactis* MG1363 was grown in the presence of 25 mM ethyl methanesulfonate (EMS) over night. This concentration of EMS allowed *L. lactis* to still grow exponentially, but at a decreased growth rate and to a lower final optical density. The exposure to EMS was stopped after 16 hours while the culture was still growing. EMS was removed by centrifugation of the culture, aspiration of the medium and re-suspending of the cells in GCDM to a final cell density of 2×10^6 cells per ml. These cells were serially transferred in emulsion 31 times.

Surfactant synthesis

One mmol Krytox 157 FS-H (MW 7500), (DuPont) was stirred under argon or nitrogen, degassed with vacuum and refilled with argon or nitrogen 2-3 times to remove oxygen. Then 2mmol thionyl chloride (Sigma-Aldrich) were added dropwise to the reaction mixture while stirring for 5minutes at 4ºC. Stirring was continued for another hour at room temperature. Then excess thionyl chloride was removed under vacuum for 30 minutes. During stirring 10 mL FC-3283 (3M, Novec) and 2 mmol O,O´-Bis(2-aminopropyl) polypropylene glycol-block-polyethylene glycol-block-polypropylene glycol (MW 900) (Jeffamine ED-900; Sigma-Aldrich) were added drop-wise. The resulting emulsion was stirred for 2 hours at room temperature. Then 20 mL FC-3283 were added and the sample was filtered through celite. Finally FC-3283 was removed under vacuum. This surfactant was used without further purification.
Although not used for the results presented here, we found that the use of 0.5% Pico-Surf™ (Dolomite Microfluidics) in HFE7500 (3M Novec) has similar emulsification properties as compared to the surfactant described above.

Proof of Principle experiment

Overnight cultures of strains NZ9000 and NZ9010 were inoculated at a ratio of 7:3 based on optical density measurements. This co-culture was serially propagated in suspension every 24 hours by preparing 1:1000 dilutions of 10 ml batch cultures. Another co-culture was propagated with the described emulsion based protocol every 48 hours for 4 transfers. Throughout the experiment dilutions of the culture were plated on GM17 or GM17 supplemented with 5 μg/ml erythromycin. NZ9010 is erythromycin resistant which allowed monitoring the fraction of NZ9010 in the mixed culture throughout the experiment.

Serial propagation in suspension

HB60 was serially propagated in 10 ml batch cultures by preparing 1:1000 dilutions every 24 hours. The fast growing revertants HB61, HB62 and HB63 are single colony isolates from three independent cultures that were propagated for

9 transfers. The number of generations generated throughout these propagations is approximately 90.
Three cultures of NZ9020 were serially propagated in 10 ml cultures as described above for up to 280 generations. Additionally 96 cultures of NZ9020 were propagated in parallel by culturing them in deep-well plates that were filled with 1.8 ml medium. Every 24 hours cultures were propagated by inoculating a deep-well plate with a 96-pin replicator that transfers roughly 1-2 µl of the fully-grown culture. Ten transfers resulted in approximately 100 generations.

Growth curve analysis

The R software package was used to analyze the growth curves from microplate experiments. The optical density (OD) measurements were background corrected for each well by subtracting the average of the first 3 reads from all values. The OD after inoculation is below the detection limit of the plate reader, which allows it to use the first values as background measurements for individual wells. Individual background correction per well has the advantage that small variations caused by irregularities in the microplate or the medium volume will be taken into account. For the determination of the growth rate the region of exponential growth was determined as values that were above the noise level of the OD measurement and below 20-50% of the maximum OD reached by each curve. The slope of the ln-transformed data was calculated as the growth rate.
The maximum OD reached was determined as the average of the three highest OD values measured after cells go into stationary phase. Growth curves that were obvious outliers, which were usually caused by gas bubbles in wells were omitted from the analysis. Per 384 well plate (384 growth curves) we usually identified less than 3 of such outliers that were omitted from data analysis.

Dry weight, cell size and fermentation end products determination

Biomass dry weight of cultures was determined by filtering 4 ml of cell culture through a dried, and pre-weighed 0.2 µm pore filter using a vacuum pump and subsequent drying at 60°C until filters reached a stable weight.
Bacterial cell size and number was determined in a Multisizer 3 (Beckman-Coulter), which was used with a 30 µm aperture according to the manufacturers instructions.
The extracellular concentration of glucose, lactate, formate, acetate, pyruvate, succinate and ethanol was quantified by HPLC analysis of fermentation supernatants obtained by filtration through a 0.2 µm polyethersulfone (PES) filter (VWR International B.V., Amsterdam, The Netherlands). Separation and quantification of the compounds of interest was achieved using an isocratic flow through an aminex ion-exclusion column using a previously described set up (14). The carbon flux towards lactate was estimated as the fraction of carbon [in mM] in the metabolic end-products lactate, acetate and formate: Fraction of lactate = (3× [lactate])/(3×[lactate] + 2×[acetate] + [formate]).

Acidification measurements

Cells were pre-cultured for 16 hours and propagated 1:20 in the same medium. When mid-logarithmic, cells were washed once in saline supplemented with 5µg/ml chloramphenicol and re-suspended in CDM medium that was diluted with four parts of saline and supplemented with 10 µM of 5-(6)-Carboxyfluorescein (#21877, Sigma-Aldrich) and 5 µg/ml chloramphenicol. Multiple wells of a black microplate with transparent bottom were filled with 190µl of the cell suspension and the optical density was determined. Subsequently 10 µl of 100mM glucose solution were added to each well (resulting in a concentration of 5 mM glucose) and fluorescence emission at 520 nm (Excitation 485 nm) was measured in regular intervals for 2 hours in a microplate reader (Fluorostar, BMG LABTECH GmbH, Ortenberg, Germany).
This cell suspension was weakly buffered and allowed acidification measurements based on the decreasing fluorescence intensity of the pH-dependent indicator carboxy-fluoresceine. The addition of chloramphenicol prevents translation and therefore the measured acidification rate is a measure for the glycolytic flux with the protein machinery present during the growth phase in which cells were harvested. Acidification was plotted as the slope of the linear decrease in fluorescence corrected for the optical density (fluorescence in arbitrary units/minute/OD600) and normalized to strain MG1363.

Protein determination

To determine total protein content, 1000 µl of fully-grown cultures were washed two times with saline and re-suspended in 200 µl saline. 50 µl of 10% SDS were added and subsequently incubated at 90˚C for one hour. Total protein was then determined by using the BCA protein assay Kit (Sigma-Aldrich) according to the manufacturers specifications. The 1000 µl of culture used were obtained by pooling 4 times 250 µl of independent cultures that were grown in a 96-well microplate in a plate reader.

Genome re-sequencing

Microbial DNA for genome sequencing was isolated from 3×10^9 cells of an overnight culture with the DNeasy Blood & Tissue kit (Quiagen) according to the manufacturers instructions . Sequencing of genomic DNA was performed on an Illumina HiSeq2000 platform as described earlier (15), with the deviation that the enrichment step was omitted and the libraries were sequenced as single 101 bp reads. Sequencing resulted in 8834988, 20378452 and 9108362 reads for strains HB60, HB61 and HB63 respectively, which corresponds to an average sequence coverage of 318.9, 718.4 and 332 respectively. Sequence analysis was done with the Breseq Software package (16) using standard settings and the MG1363 genome as a reference (GenBank file: NC_009004). The call of mutations was based on comparison with the sequencing data obtained from the re-sequencing of the original strain that was used to start all experiments, designated *L. lactis* Gen0. The insertion of IS905 upstream of *ptnABCD* and upstream of *glcU* was confirmed by PCR amplification and Sanger amplicon sequencing of the insertion loci.

The sequencing data of strains HB60, HB61 and HB63 is deposited in the NCBI Sequence Read Archive (SRA) under the project number SRP017852. The sequencing data of strain Gen0, is deposited under the accession number SRS385784.

SI Appendix: References

1. Pfeiffer T, Schuster S, Bonhoeffer S (2001) Cooperation and competition in the evolution of ATP-producing pathways. *Science* 292:504–7.

2. Thomas TD, Ellwood DC, Longyear VM (1979) Change from homo- to heterolactic fermentation by *Streptococcus lactis* resulting from glucose limitation in anaerobic chemostat cultures. *Journal of bacteriology* 138:109–17.

3. Vemuri GN, Altman E, Sangurdekar DP, Khodursky AB, Eiteman MA (2006) Overflow metabolism in *Escherichia coli* during steady-state growth: transcriptional regulation and effect of the redox ratio. *Applied and environmental microbiology* 72:3653–61.

4. Warburg O (1956) On the Origin of Cancer Cells. *Science* 123:309–314.

5. Novak M, Pfeiffer T, Lenski RE, Sauer U, Bonhoeffer S (2006) Experimental tests for an evolutionary trade-off between growth rate and yield in *E. coli*. *The American naturalist* 168:242–51.

6. MacLean RC (2008) The tragedy of the commons in microbial populations: insights from theoretical, comparative and experimental studies. *Heredity* 100:233–9.

7. Merico A, Sulo P, Piskur J, Compagno C (2007) Fermentative lifestyle in yeasts belonging to the *Saccharomyces* complex. *The FEBS journal* 274:976–89.

8. Bongers RS et al. (2003) IS*981*-Mediated Adaptive Evolution Recovers Lactate Production by *ldhB* Transcription Activation in a Lactate Dehydrogenase-Deficient Strain of *Lactococcus lactis*. *Journal of Bacteriology* 185:4499–4507.

9. Gaspar P et al. (2007) The lactate dehydrogenases encoded by the *ldh* and *ldhB* genes in *Lactococcus lactis* exhibit distinct regulation and catalytic properties - comparative modeling to probe the molecular basis. *The FEBS journal* 274:5924–36.

10. Dodd HM, Horn N, Gasson MJ (1994) Characterization of IS*905*, a new multicopy insertion sequence identified in lactococci. *Journal of bacteriology* 176:3393–6.

11. Pool WA, Neves AR, Kok J, Santos H, Kuipers OP (2006) Natural sweetening of food products by engineering *Lactococcus lactis* for glucose production. *Metabolic engineering* 8:456–64.

12. Kuipers OP, De Ruyter PGGA, Kleerebezem M, De Vos WM (1998) Quorum sensing-controlled gene expression in lactic acid bacteria. *Journal of Biotechnology* 64:15–21.

13. Youk H, Van Oudenaarden A (2009) Growth landscape formed by perception and import of glucose in yeast. *Nature* 462:875–9.

14. Goel A, Santos F, De Vos WM, Teusink B, Molenaar D (2012) Standardized Assay Medium To Measure *Lactococcus lactis* Enzyme Activities while Mimicking Intracellular Conditions. *Applied and environmental microbiology* 78:134–43.

15. Duns G et al. (2012) Targeted exome sequencing in clear cell renal cell carcinoma tumors suggests aberrant chromatin regulation as a crucial step in ccRCC development. *Human mutation* 33:1059–62.

16. Barrick JE et al. (2009) Genome evolution and adaptation in a long-term experiment with *Escherichia coli*. *Nature* 461:1243–7.